Progress in Natural Science: Materials International 2012;22(4):265–272

Chinese Materials Research Society

Progress in Natural Science: Materials International

www.elsevier.com/locate/pnsmi
www.sciencedirect.com

ORIGINAL RESEARCH

Synergistic effect between ceria and tungsten oxide on WO_3–CeO_2–TiO_2 catalysts for NH_3-SCR reaction

Lei Chen[a], Duan Weng[a,*], Zhichun Si[b], Xiaodong Wu[a,c]

[a] *State Key Lab of New Ceramics and Fine Processing, Department of Materials Science and Engineering, Tsinghua University, Beijing 100084, China*
[b] *Advanced Materials Institute, Graduate School at Shenzhen, Tsinghua University, Shenzhen 518055, China*
[c] *Yangtze Delta Region Institute of Tsinghua University, Zhejiang 314000, China*

Received 27 April 2012; accepted 10 June 2012
Available online 14 August 2012

KEYWORDS

NH_3-SCR;
WO_3–CeO_2–TiO_2 catalysts;
Oxygen activation;
Acid sites

Abstract WO_3–CeO_2–TiO_2 catalysts for NO (nitrogen monoxide) reduction by ammonia were prepared by a sol–gel method. The catalysts were characterized by BET, XRD, Raman, NH_3/NO adsorption and H_2-TPR to investigate the relationships among the catalyst composition, structure, redox property, acidity and deNO_x activity. WO_3–CeO_2–TiO_2 catalysts show a high activity in a broad temperature range of 200–480 °C. The low-temperature activity of catalysts is sensitive to the catalyst composition especially under low-O_2-content atmospheres. It may be related to the synergistic effect between CeO_x and WO_x in the catalysts. On one hand, the interaction between ceria and tungsten oxide promotes the activation of gaseous oxygen to compensate the lattice oxygen consumed in NH_3-SCR (selective catalytic reduction) reaction at low temperatures. Meanwhile, the Brønsted acid sites mainly arise from tungsten oxides, Lewis acid sites mainly arise from ceria. Both of the Brønsted and Lewis acid sites facilitate the adsorption of NH_3 on catalysts and improve the stability of the adsorbed ammonia species, which are beneficial to the NH_3-SCR reaction.

1. Introduction

Nitrogen oxides (NO_x) remain a major ecological problem since they can cause acid rain and photochemical smog. NH_3-SCR (selective catalysis reduction) is the most widely used technology for reducing NO_x emissions from automobile and stationary sources [1–3]. The general NH_3-SCR reaction is as following:

$$4NH_3+4NO+O_2 \rightarrow 4N_2+6H_2O \quad (1)$$

*Corresponding author.
E-mail addresses: lchen11@mails.tsinghua.edu.cn (L. Chen), duanweng@mail.tsinghua.edu.cn (D. Weng).

Peer review under responsibility of Chinese Materials Research Society.

Production and hosting by Elsevier

1002-0071 © 2012 Chinese Materials Research Society. Production and hosting by Elsevier Ltd. All rights reserved.
http://dx.doi.org/10.1016/j.pnsc.2012.07.004

V_2O_5–$WO_3(MoO_3)$–TiO_2 is the most commonly used commercial deNO_x catalyst due to its high activity, high selectivity and high resistance to SO_2. However, some disadvantages, such as the narrow working windows (generally located at 300–400 °C) and high toxicity of vanadium inhibit their further applications. Therefore, novel catalysts for replacement of V_2O_5–$WO_3(MoO_3)$–TiO_2 catalyst have attracted much attention in recent years.

CeO_2 is well known for its oxygen storage capacity and high redox ability shifting between Ce^{4+} and Ce^{3+} [4–6]. CeO_2 is also considered as the active component in SCR reaction due to its ability of enhancing the oxidation of NO to NO_2 [7]. Recently, CeO_2 based SCR catalysts have been extensively studied, such as Ce–Cu–Ti [8], Ce-activated carbon fiber [9], Ce-carbon nanotubes [10], Ce-titanium nanotubes [11], Ce-ZSM5 [12], Mn–Ce [13,14], Ce–Al [15], Ce–Zr–Ni–SO_4^{2-} [16], Cr–Ce [17] and Mn–Ce–Ti [18,19]. Ceria based catalysts containing acidic components (such as SO_4^{2-} [16] and WO_3 [20]) show high NH_3-SCR activity and N_2 selectivity in a wide temperature window. According to Chen et al. [21], the strong interaction between Ce and W results in more Ce^{3+}, which creates charge imbalance facilitating more chemisorbed oxygen on the surface of catalysts. The chemisorbed oxygen is considered as the most active oxygen for NO_2 formation in the "fast SCR" reaction in which the reaction rate is much faster than that in standard NH_3-SCR reaction [22]. Hoewever, Djerad et al. [23] proved that the O_2 concentration strongly affects the low-temperature (150–275 °C) NH_3-SCR activity of V_2O_5–WO_3/TiO_2 via converting part of NO to NO_2. Especially, SCR catalytic reactor for deNO_x of nitric acid plants and some chemical process are always installed in very low oxygen concentrations around 2–3% [24]. However, to our best knowledge, the effects of ceria on the NH_3-SCR activities of catalysts in various oxygen concentrations, which is important for obtaining catalyst across a broad range of conditions and reducing the dosage of ceria in catalysts, have been fewly studied.

In the present work, the WO_3–CeO_2–TiO_2 catalysts containing different amounts of ceria were prepared by a sol–gel method to provide catalysts with high deNO_x performances in various O_2 containing conditions. The synergistic effects between ceria and tungsten on redox behaviors, adsorptive properties and NH_3-SCR activity of catalysts were studied.

2. Experimental

2.1. Catalyst preparation

The catalysts were prepared by a sol–gel method. Ammonium paratungstate (AR, Beijing Chem. Plant), cerium nitrate hexahydrate (AR, Aladdin), citric acid (AR, Aladdin), nitric acid (AR, Beijing Chem. Plant), tetrabutyl titanate (AR, Beijing Chem. Plant) were all analytical reagents. The tetrabutyl titanate was added dropwise into the nitric acid and citric acid mixed aqueous solution. The ammonium paratungstate, cerium nitrate hexahydrate was added into the solution. The molar ratio of metal components (W, Ce and Ti) to citric acid to nitric acid is 1:1.5:1.5. The solutions were stirred and heated for 3 h to form a gel, and then the gels were dried at 110 °C for 12 h and calcined in a maffel furnace at 600 °C for 3 h. The number x in the catalysts (WCe_xTi, Ce_xTi) represented the molar percentage of CeO_2, and the WO_3 was 10 wt% in all the W-containing catalysts.

2.2. Catalyst characterization

The powder X-ray diffraction (XRD) experiments were performed on a Japan science D/mas-RB diffractometer employing Cu Kα radiation ($\lambda = 0.15418$ nm). The X-ray tube was operated at 40 kV and 120 mA. The X-ray powder diffractogram was recorded at 0.02° intervals in the range of $10° < 2\theta < 80°$. The identification of the phases was made with the help of JCPDS cards (Joint Committee on Powder Diffraction Standards). The mean crystallite sizes were calculated by Scherer formula.

The Raman spectra were obtained with a Renishaw RM2000 Confocal Raman spectrometer at room temperature and atmospheric pressure. 633 nm was used as the exciting source from an argon ion laser. The laser beam was focused onto an area 0.1 mm × 0.1 mm in size of the sample surface. The wavenumber values of the Raman spectra are accurate to 1 cm^{-1}.

The specific surface areas of the samples were measured using the N_2 physisorption at −196 °C by Brunauer–Emmett–Teller (BET) method using an automatic surface analyzer (F-sorb 3400). The samples were degassed in flowing N_2 at 200 °C for 2 h.

A thermo Nicolet 6700 Fourier Transform Infrared (FTIR) spectrometer was equipped with a high-temperature environmental cell fitted with KBr window. In situ FTIR spectra of adsorbed species, which arise from NH_3/NO+O_2 adsorption, were recorded in the range of 4000–650 cm^{-1}. Prior to the adsorption, the sample was placed in a crucible located in a high-temperature cell and heated up to 500 °C in a 20% (v/v) O_2/N_2 flow mixture with a total flow of 100 ml for 30 min to remove traces of organic residues. After that, the sample was cooled down to the corresponding temperature and was flushed by 100 ml min^{-1} N_2 for 30 min to remove the physisorbed molecules for background collection. Then, a gas mixture containing 1000 ppm NH_3 or 1000 ppm NO in 5% O_2+N_2 with a total flow rate of 100 ml/min passed through the sample for 60 min. After purging the weakly adsorbed or gaseous NH_3/NO_x molecules by N_2 flow for 30 min, the FTIR spectra of adsorbed species on catalysts were collected simultaneously.

H_2-TPR experiments were conducted on a Mecromeritics Autochem ‖ 2920 chemisorption analyzer using 50 mg of the samples. Samples were preheated at 500 °C for 30 min in He flow. The temperature was increased from 50 to 1000 °C at a heating rate of 10 °C min^{-1} with 10% H_2/Ar gases. The H_2 consumption was recorded continuously.

2.3. Activity measurements

The catalytic activity measurement for reduction of NO by ammonia (NH_3-SCR) with excess oxygen was carried out in a fixed bed reactor made of quartz glass tube. 0.2 g catalysts were diluted to 1 ml by silica sand. The reaction gas mixture simulating diesel engine exhaust gases consisted of 500 ppm NO, 500 ppm NH_3, variable O_2 from 0% to 10%, and N_2 in balance. The NO_x conversion was measured after 30 min stable at various temperatures. The total flow of the gas mixture was 500 mL min^{-1} at a gas hourly space velocity (GHSV) of 30,000 h^{-1}. The concentrations of nitrogen oxides

and ammonia were measured at 120 °C by a Thermo Nicolet 380 FTIR spectrometer equipped with 2 m path-length sample cell (250 ml volume). The gas path from the reactor to FTIR spectrometer was maintained at a constant temperature of 120 °C to avoid NH_4NO_2/NH_4NO_3 deposition. The NO_x conversions were calculated as follows:

$$NO_x \text{ conversion } (\%) = \frac{NO_{in} - NO_{out} - NO_{2out} - 2N_2O_{out}}{NO_{in}} \times 100 \quad (2)$$

3. Results

3.1. Catalytic activity

The NH_3-SCR activities of catalysts measured in 5% O_2 are shown in Fig. 1. Generally, the activities of tri-component catalysts ($WCe_{10}Ti$ and $WCe_{80}Ti$) are remarkably higher than those of bi-component catalysts (WTi, $Ce_{10}Ti$ and $Ce_{80}Ti$). For the bi-component catalysts, WTi catalyst mainly presents significant NO_x conversion at temperatures higher than 350 °C while $Ce_{10}Ti$ catalyst only shows high NO_x conversions in a narrow temperature region of 280–360 °C. As the content of CeO_2 increases, the NO_x conversion of $Ce_{80}Ti$ catalyst decreases obviously and is even below zero due to the over oxidation of NH_3 to NO_x at the temperatures above 400 °C.

For the tri-component catalysts, the NH_3-SCR activity of the catalysts show little changes as the CeO_2 content increases from 10% to 80%, The CeO_2-rich catalyst shows superior low-temperature activity, while the TiO_2-rich catalyst has higher high-temperature activity. It is noticed that WO_3 modification improves the NH_3-SCR activity of CeO_2–TiO_2 in the whole temperature range.

The effect of O_2 concentration on the NO_x conversions of the WO_3–CeO_2–TiO_2 catalysts at 200 °C is presented in Fig. 2. All the catalysts presented low NH_3-SCR activities in absence of oxygen and their activities increased with increasing O_2 concentration in the reaction atmosphere, indicating the importance of O_2 in NH_3-SCR reactions, especially at low temperatures ranging from 150 to 275 °C [23]. The WTi catalyst showed a minor increase of NO_x conversions as the oxygen concentration increased from 0% to 10%, which suggests that WTi catalyst is not sensitive to the oxygen concentration. For the $Ce_{80}Ti$ and $WCe_{80}Ti$ catalyst, the NH_3-SCR activity increases sharply with the introduction of a low concentration of oxygen and shows little changes when the oxygen concentration was higher than 1%. Comparatively, the NH_3-SCR activities of $Ce_{10}Ti$ and $WCe_{10}Ti$ kept increasing even when the oxygen concentration increased up to 10%.

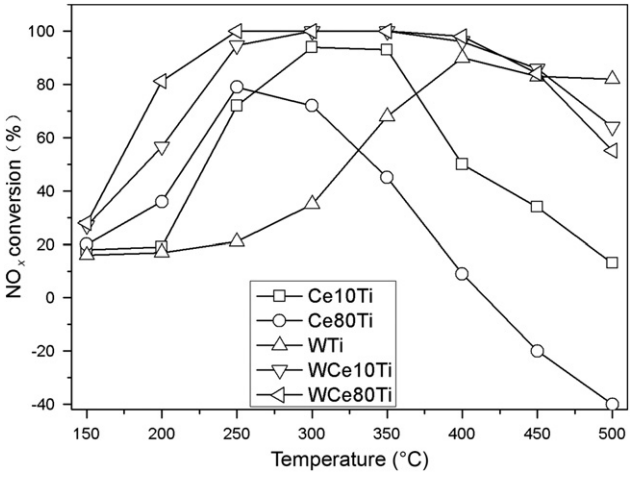

Fig. 1 NO_x conversion over the catalysts as a function of temperature. Reaction conditions: [NO]=[NH_3]=500 ppm, [O_2] =5%, N_2 balances, GHSV 30,000 h^{-1}.

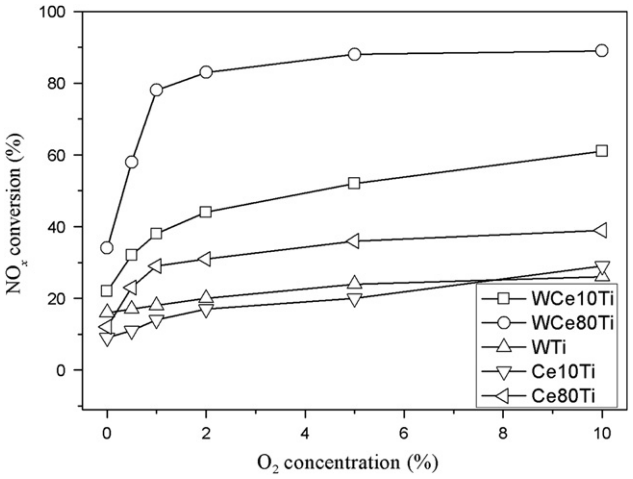

Fig. 2 NH_3-SCR activities of the catalysts at 200 °C as a function of the O_2 concentration in the reaction gas mixture. Reaction conditions: [NO]=[NH_3]=500 ppm, balance N_2, GHSV 30,000 h^{-1}.

According to the published reports [25,26], lattice oxygen of catalysts usually participate in NH_3-SCR reactions in absence of oxygen. The NO_x conversions of $Ce_{80}Ti$ and $WCe_{80}Ti$ increased more pronouncedly than those of $Ce_{10}Ti$ and $WCe_{10}Ti$ when a small amount of oxygen was introduced, indicating that the high ceria content in WO_3–CeO_2–TiO_2 catalysts helps to utilize the gaseous oxygen to make up the lattice oxygen consumed in NH_3-SCR reaction at low temperatures.

3.2. Structural property

The XRD patterns of the catalysts prepared by the sol–gel method are shown in Fig. 3. The dominant phase of $Ce_{10}Ti$, WTi and $Ce_{10}WTi$ catalysts is anatase TiO_2, while that of $Ce_{80}Ti$ and $Ce_{80}WTi$ is cubic ceria. Tungsten species are not detected in XRD patterns. The reason could be that tungsten oxide is highly dispersed or form a solid solution with dominant phase. The compositions, mean crystallite sizes and BET surface areas of the catalysts are shown in Table 1. It is noted that the addition of tungsten oxide on CeO_2–TiO_2 catalysts inhibited the growth of titania and ceria crystallites. The BET surface areas of catalysts were ranged between 57 and 70 m^2/g, which should not bring any obvious difference of the catalytic activity.

The Raman spectra of the catalysts are presented in Fig. 4. The bands at 248, 403, 462, 520, 614 and 636 cm^{-1} were detected, and the results are shown in Fig. 4(a). The adsorption bands at 462–452 cm^{-1} for the ceria rich samples ($Ce_{80}Ti$

and $WCe_{80}Ti$) are assigned to the Raman active F_{2g} mode of CeO_2 cubic lattice [27]. The F_{2g} band of $WCe_{80}Ti$ catalyst becomes broader with a blue shift around 10 cm^{-1} compared with $Ce_{80}Ti$. The bands at 399–403, 512–520 and 636 cm^{-1}, which were distinctly detected on $Ce_{10}Ti$ and WTi samples, could be assigned to B_{1g}, A_{1g}/B_{1g} and E_g modes of anatase TiO_2, respectively [28]. The small band at 248 cm^{-1} is attributed to the band of rutile. Generally, the band intensity of tri-component catalysts is much lower than those of the bi-component catalysts.

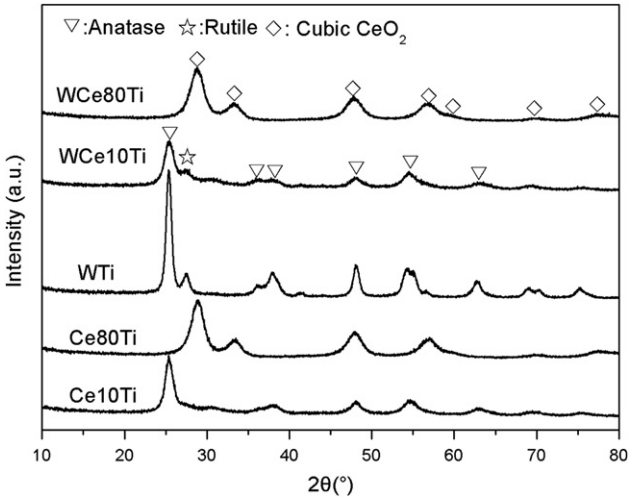

Fig. 3 XRD patterns of the catalysts.

Table 1 The composition and structural features of the catalysts.

Catalyst	Composition (wt%)			S_{BET} (m^2g^{-1})	Crystaillite size (nm)
	WO_3	CeO_2	TiO_2		
$Ce_{10}Ti$	–	10	90	66	7.0[a]
$Ce_{80}Ti$	–	80	20	62	4.8[b]
WTi	10	–	90	62	10.6[a]
$WCe_{10}Ti$	10	10	80	70	5.4[a]
$WCe_{80}Ti$	10	80	10	57	4.4[b]

[a]The dominant phase is anatase TiO_2.
[b]The dominant phase is cubic ceria.

The high wavenumbers of Raman spectra are presented in Fig. 4(b). One distinct band at 997 cm^{-1} was detected in the WTi catalyst which is related to tetrahedral coordinated WO_x species arising from highly dispersed WO_x species [29]. There were no obvious bands corresponding to the tungsten oxide species in tri-component catalysts.

3.3. *Redox property*

H_2-TPR is a widely used technique in the study of the redox properties of the catalysts. The H_2-TPR profiles of the prepared catalysts are shown in Fig. 5. Two reduction peaks at 441 and 554 °C appear in the $Ce_{10}Ti$ sample, attributing to the surface oxygen reduction of CeO_2 [21]. The reduction process could be interpreted as a stepwise reduction: the first peak is attributed to the reduction of Ce^{4+}–O–Ce^{4+}, and the second peak corresponds to the reduction of Ce^{3+}–O–Ce^{4+} [30,31]. The H_2-TPR profile of $Ce_{80}Ti$ shows an overlapped reduction peak centered at 533 °C, attributing to the reduction of surface/subsurface oxygen. It can be seen that the peak area of the $WCe_{80}Ti$ catalyst is larger than that of $Ce_{80}Ti$, which implies that the introduction of tungsten oxide results in more reducible subsurface and bulk oxygen in the tri-component catalysts. Additionally, the H_2 peak area of surface oxygen reduction is increased significantly as increasing the CeO_2 content, indicating that the surface oxygen mainly arises from ceria [32].

3.4. *Ammonia adsorption*

The *in-situ* DRIFT spectra of the catalysts arising from contact with NH_3 at 200 and 300 °C were shown in Fig. 6. In Fig. 6(a), the strong bands at 1595 and 1170 cm^{-1} are observed for all the samples, which can be attributed to the σ_{as} NH_3 and σ_s NH_3 vibrations on Lewis acid sites [33,34]. The bands at 1670 and 1425 cm^{-1} are attributed to the σ_s and σ_{as} vibrations of NH_4^+ on the Brønsted acid sites [35,36]. The acid concentration and strength of Brønsted/Lewis acid sites can be

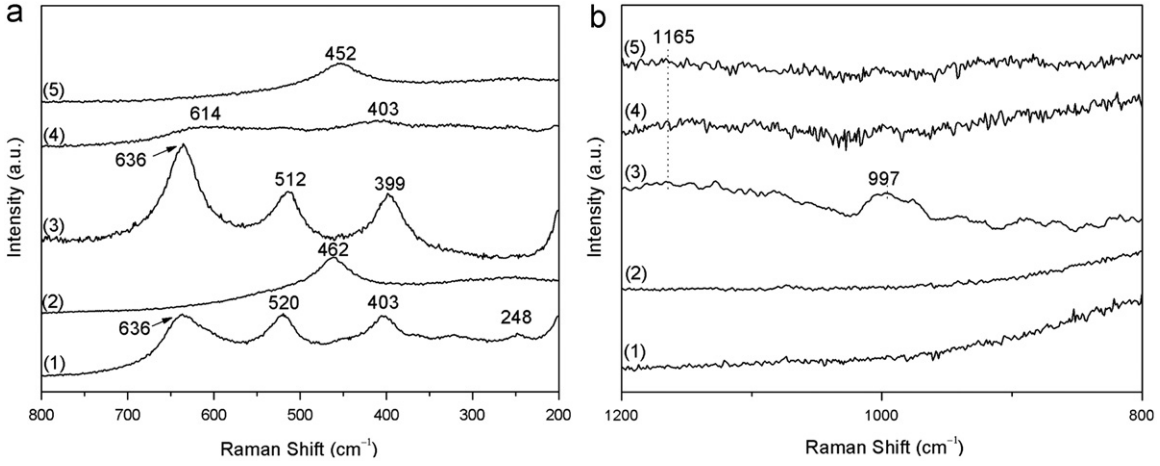

Fig. 4 Raman spectra of the (1) $Ce_{10}Ti$, (2) $Ce_{80}Ti$, (3) WTi, (4) $WCe_{10}Ti$ and (5) $WCe_{80}Ti$ catalysts at (a) 800–200 cm^{-1} and (b) 1200–800 cm^{-1}.

determined by the band area and band position of the σ_s NH_3 and σ_{as} NH_4^+ respectively, i.e. bands at higher wavenumbers indicate the stronger acidity, and larger band area means the higher concentration of acid sites. In $Ce_{10}Ti$ and $Ce_{80}Ti$ catalysts, the bands assigned to Lewis acid sites are predominated. The adsorption band of WTi catalyst could mainly assigned to the Brønsted acid sites. The band at 1571 cm^{-1}, which is detected in tri-component catalysts, can be assigned to the intermediate oxidation of ammonia [7,37]. In N–H band region, bands at 3369 and 3250 cm^{-1} could be detected. Basically, it can be seen by comparison between $Ce_{10}Ti$–$Ce_{80}Ti$ and $WCe_{10}Ti$–$WCe_{80}Ti$ catalysts that the strength of the Lewis acid sites increases with the increase of the CeO_2 content. The introduction of WO_x remarkably increases the amount of Brønsted acid sites. Thus, Brønsted acid sites are mainly arising from tungsten oxides, and the Lewis acid sites mainly depend on the content of CeO_2.

The *in-situ* DRIFT spectra of the catalysts arising from contact of NH_3 at 300 °C are shown in Fig. 6(b). At the high temperature, all the Lewis and Brønsted acid sites peaks decrease in intensity. According to our previous study [38], the Lewis acidity facilitates the low-temperature NH_3-SCR reaction, but leads to accelerated ammonia consumption. This may explain the low NH_3-SCR activity and N_2 selectivity of the W-free catalysts ($Ce_{10}Ti$ and $Ce_{80}Ti$) at high temperatures.

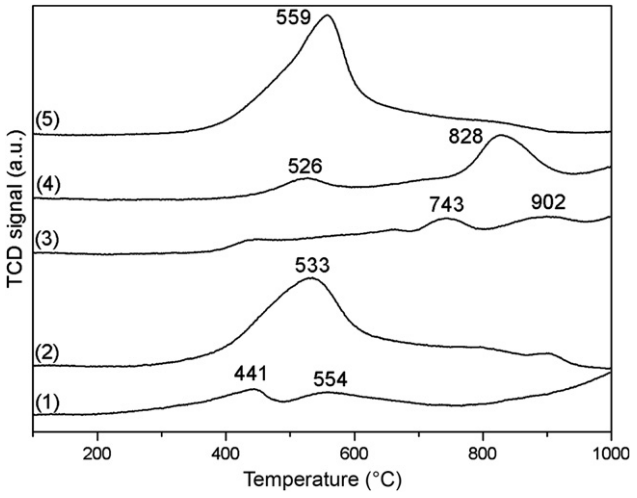

Fig. 5 H_2-TPR profiles of the (1) $Ce_{10}Ti$, (2) $Ce_{80}Ti$, (3) WTi, (4) $WCe_{10}Ti$ and (5) $WCe_{80}Ti$ catalysts.

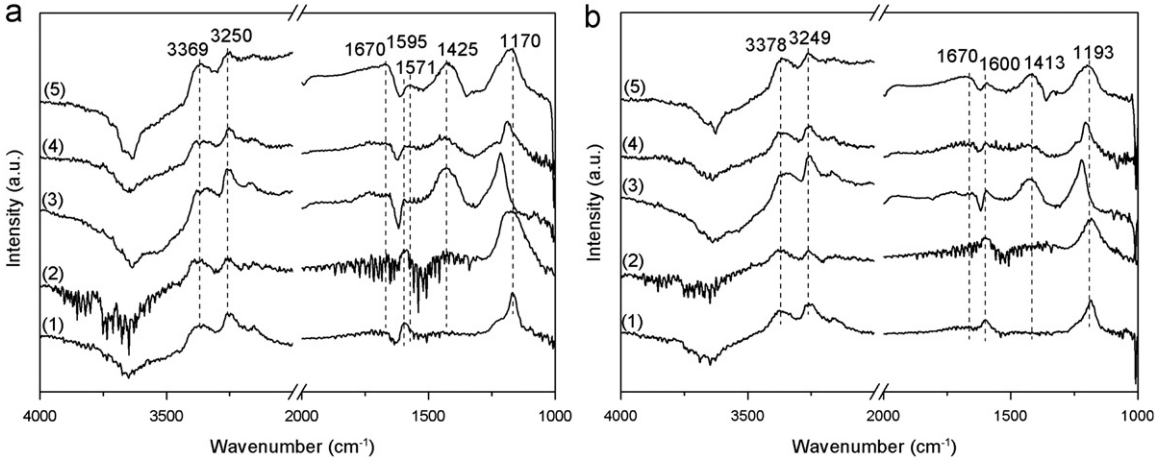

Fig. 6 DRIFT spectra of adsorbed species on the (1) $Ce_{10}Ti$, (2) $Ce_{80}Ti$, (3) WTi, (4) $WCe_{10}Ti$ and (5) $WCe_{80}Ti$ catalysts arising from contact with 1000 ppm NH_3 at (a) 200 °C and (b) 300 °C.

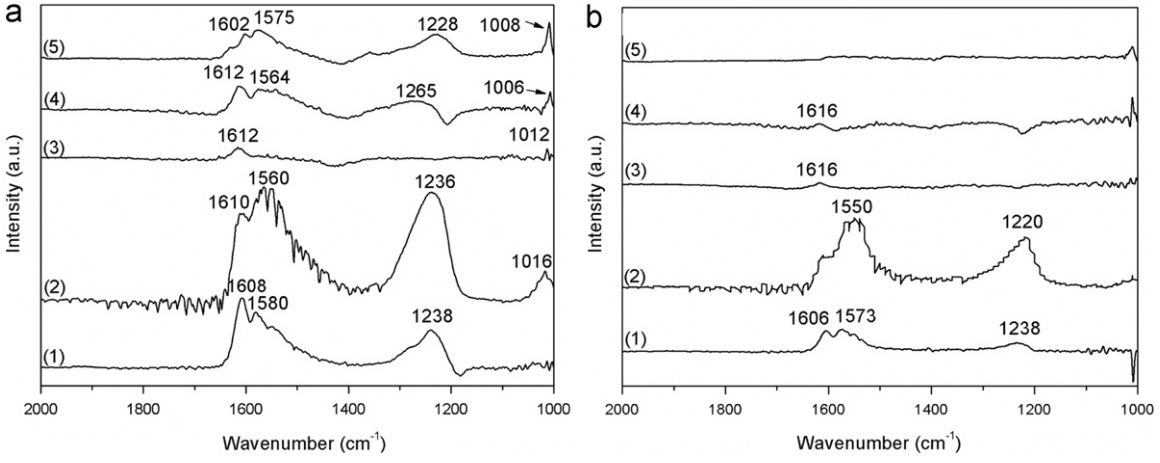

Fig. 7 DRIFT spectra of adsorbed species on the (1) $Ce_{10}Ti$, (2) $Ce_{80}Ti$, (3) WTi, (4) $WCe_{10}Ti$ and (5) $WCe_{80}Ti$ catalysts arising from contact of 1000 ppm NO+5% O_2 at (a) 200 °C and (b) 300 °C.

3.5. $NO+O_2$ adsorption

The DRIFT spectra of the catalysts in the flow of $NO+O_2$ are shown in Fig. 7. In Fig. 7(a), the bands at 1238, 1580 and 1608 cm^{-1} were detected in $Ce_{10}Ti$ catalyst. The band at 1238 cm^{-1} could be assigned to bridging nitrates. The band at 1580 cm^{-1} might be attributed to the bidentate nitrates [7]. The band at 1608 cm^{-1} could be assigned to the asymmetric frequency of gaseous NO_2 molecules [37]. Similar bands were detected in the $Ce_{80}Ti$ catalyst with much higher bands intensity. The increase of CeO_2 addition promotes the NO_x adsorption on the surface of catalyst, which means NO_x species are prone to be adsorbed on Ce^{n+} sites. In $WCe_{10}Ti$ and $WCe_{80}Ti$ catalysts, similar bands with much lower intensity were detected, which mean that the adsorption of NO_x is inhibited by the addition of the acidic tungsten oxide.

All the NO_x adsorption bands on catalysts were weakened as the temperature increases. At 300 °C, the NO_x species almost disappeared over the tungsten-containing catalysts, indicating that NO_x adsorbed on these catalysts are quite unstable. On $Ce_{10}Ti$ and $Ce_{80}Ti$ catalysts, the bands at 1220, 1550 and 1606 cm^{-1} could still be detected, which assigned to bridged, bidentate nitrate, and the gaseous NO_2 molecules, respectively.

4. Discussion

4.1. Textural properties of catalysts

The XRD results show that the dominant phase of the catalysts is cubic ceria or anatase TiO_2. Tungsten oxide strongly inhibits the crystallization of anatase TiO_2 and leads to higher dispersion degree of ceria [39]. The Raman results revealed that in tri-component catalysts containing lots of structure defects which come from the structural and electronic interaction between cerium and tungsten. Considering the similar particle sizes of $Ce_{80}Ti$ and $WCe_{80}Ti$ in XRD results, the broadening of F_{2g} band over $WCe_{80}Ti$ (452 cm^{-1}) might arise from the oxygen vacancies by the strong structural interaction among CeO_2, WO_3 and TiO_2 in solid solutions. Furthermore, the addition of tungsten oxides led to the relaxation of Ce–O bond as indicated by the shift of the band at 462–452 cm^{-1}, because that the Ce–O bond in Ce–O–W species may be weakened due to the electron withdrawn effect of W–O or W=O bond arising from the positive charge surplus of W^{6+} in tetrahedral coordination. However, the Ce–O bond in Ce–O–Ti species can hardly be influenced by Ti–O bond due to the negative charge surplus of octahedrally coordinated Ti^{4+}.

4.2. Redox properties and catalytic activity

Since oxygen is an essential reactant in the standard SCR reaction, the ability to provide lattice oxygen is an important factor determining the catalytic activity of the catalysts [40]. The surface oxygen has been reported to be highly active in NH_3/NO oxidation reaction due to its higher mobility than lattice oxygen, which may lead to a decrease of NH_3-SCR performance at high temperatures as a consequence of high NH_3 oxidation. From the NH_3-SCR activity and H_2-TPR results, ceria helps to utilize the gaseous oxygen to make up the lattice oxygen consumed in NH_3-SCR reaction at low temperatures. Therefore, the low-temperature NH_3-SCR activity of catalysts is dependent on the ceria content especially under low O_2 concentrate conditions. From the H_2-TPR curves, the surface oxygen mainly arises from ceria and consequently the CeO_2–TiO_2 bi-component catalysts only present low NH_3-SCR activity at temperatures higher than 300 °C. However, the introduction of tungsten oxide to the CeO_2–TiO_2 solid solution inhibits the reduction of surface oxygen but results in more reducible bulk oxygen in the catalysts. The increased structural defects, the relaxed Ce–O bond and the reduced crystalline size of WO_x–CeO_x–TiO_x solid solution may facilitate the mobility of lattice oxygen of catalysts.

4.3. Acidity, NO_x adsorption and SCR activity

The results of NH_3/NO adsorption indicate that the introduction of WO_x remarkably increases the intensity of Brønsted acid sites, while Lewis acid sites mainly depend on the content of CeO_2. According to the literature reported [2,41], catalysts with high acidity and moderate redox properties may present remarkable high-temperature (>400 °C) NH_3-SCR performances. Catalysts with high acidity may help to reduce the ammonia oxidation and improve ammonia adsorption on catalysts at high temperatures. The NH_3 adsorption results showed that most of Brønsted acid sites arise from tungsten oxide via the reaction (Eq. (3)). Brønsted acid sites have no redox properties and may help to inhibit the NH_3 oxidation at high temperatures [38]. Furthermore, the introduction of tungsten oxide into the CeO_2–TiO_2 solid solution will inhibit the reduction of surface oxygen and thereby inhibit the ammonia oxidation. Therefore, WO_3–CeO_2–TiO_2 catalysts can present high NH_3-SCR performance in a wide temperature window of 200–480 °C.

$$-W=O+NH_3 \rightarrow -W-O-NH_4^+ \quad (3)$$

$$Ce^{4+}-O+NO \rightarrow Ce^{3+}-NO_2 \quad (4)$$

$$-W-O-NH^{4+}+O^*+-NO \rightarrow -NO_2 \quad (5)$$

$$-NO_2+O^* \rightarrow -NO_3 \quad (6)$$

$$2NH_3+NO_2+NO \rightarrow 2N_2+3H_2O \quad (7)$$

In the present study, NO_x are prone to adsorbed on the ceria-related sites while tungsten helps to reduce the ammonium nitrate deposition on catalysts. The structural and electronic interactions among CeO_x, WO_x and TiO_x lead to the improved mobility of lattice oxygen, facilitating the formation of nitrate species on catalysts (Eqs. (4)–(6)), which may be one aspect for the higher SCR activity of tri-component catalysts than those bi-component catalysts because that the nitrate can react with NO to generate NO_2. According to Chen et al. [37], the SCR reaction over WO_3–CeO_2–TiO_2 catalysts follows the E–R mechanism: the reaction between NO_x and absorbed ammonia are predominate, while that between ammonia and absorbed nitrogen oxides species only occurs between ammonia and NO_2. NO_x adsorption was reported to accelerate the NH_3-SCR reaction over catalyst via the "fast SCR" [22] (Eq. (7)).

It is noticeable that both $Ce_{80}Ti$ and WTi catalysts present low NH_3-SCR activity, indicating that both the Lewis and

Brønsted acid sites arising from ceria and tungsten oxides play important roles in SCR reaction over the tri-component catalysts. The NO_x species may participate in the SCR reaction via reoxidizing the Ce^{n+}-related active sites, and W plays a promoter by improving the NO_x species desorption and decomposition. At low temperatures, NH_3 and NO_x are more likely to be adsorbed on surface of catalysts rather than O_2. The oxygen activation during SCR reaction, especially in low oxygen conditions, may be the rate-determining step [23].

5. Conclusions

WO_3–CeO_2–TiO_2 catalysts synthesized by the sol–gel method present high NH_3-SCR performances in a wide temperature window of 200–480 °C. Both the redox and acidic properties (Lewis and Brønsted acid sites) of catalysts play important roles in the SCR reaction. The increased structural defects, the relaxed Ce–O bond and the reduced crystalline size of WO_x–CeO_x–TiO_x mixed oxides arising from the strong structural and electronic interactions, may activate gaseous oxygen to compensate the lattice oxygen consumed in NH_3-SCR reaction at low temperatures and thereby results in the high SCR activity of WO_3–CeO_2–TiO_2 catalysts especially in low oxygen content conditions.

Acknowledgments

We would like to acknowledge the Ministry of Science and Technology, PR China for financial support of Project 2010CB732304 and Science and Technology Department of Zhejiang Province Project 2011C31010.

References

[1] P. Forzatti, Environmental catalysis for stationary applications, Catalysis Today 62 (2000) 51–65.
[2] G. Busca, L. Liette, G. Ramis, et al., Chemical and mechanistic aspects of the selective catalytic reduction of NO_x by ammonia over oxide catalysts: a review, Applied Catalysis B: Environmental 18 (1998) 1–36.
[3] R.M. Heck, Catalytic abatement of nitrogen oxides—stationary applications, Catalysis Today 53 (1999) 519–523.
[4] L. Chen, J.H. Li, M.F. Ge, et al., Enhanced activity of tungsten modified CeO_2/TiO_2 for selective catalytic reduction of NO_x with ammonia, Catalysis Today 153 (2010) 77–83.
[5] Y. Huang, Z.Q. Tong, B. Wu, et al., Low temperature selective catalytic reduction of NO by ammonia over V_2O_5–CeO_2/TiO_2, Journal of Fuel Chemistry and Technology 36 (2008) 616–620.
[6] M.F. Luo, J. Chen, L.S. Chen, et al., Structure and redox properties of $Ce_xTi_1-_xO_2$ solid solution, Chemistry of Materials 13 (2001) 197–202.
[7] G. Qi, R.T. Yang, R. Chang, MnO_x–CeO_2 mixed oxides prepared by co-precipitation for selective catalytic reduction of NO with NH_3 at low temperatures, Applied Catalysis B: Environmental 51 (2004) 93–106.
[8] X. Gao, X.S. Du, W.C. Li, et al., A Ce–Cu–Ti oxide catalyst for the selective catalytic reduction of NO with NH_3, Catalysis Communications 12 (2010) 255–258.
[9] L.L. Zhu, B.C. Huang, W.H. Wang, et al., Low-temperature SCR of NO with NH_3 over CeO_2 supported on modified activated carbon fibers, Catalysis Communications 12 (2011) 394–398.
[10] X.B. Chen, S. Gao, H.Q. Wang, et al., Selective catalytic reduction of NO over carbon nanotubes supported CeO_2, Catalysis Communications 14 (2011) 1–5.
[11] H.Q. Wang, X.B. Chen, X.L. Weng, et al., Enhanced catalytic activity for selective catalytic reduction of NO over titanium nanotube-confined CeO_2 catalyst, Catalysis Communications 12 (2011) 1042–1045.
[12] W.E.J. van Kooten, B. Liang, H.C. Krijnsen, et al., Ce-ZSM-5 catalysts for the selective catalytic reduction of NO_x in stationary diesel exhaust gas, Applied Catalysis B: Environmental 21 (1999) 203–213.
[13] F. Eigenmann, M. Maciejewski, A. Baiker, Selective reduction of NO by NH3 over manganese–cerium mixed oxides: relation between adsorption, redox and catalytic behavior, Applied Catalysis B: Environmental 62 (2006) 311–318.
[14] G. Qi, R.T. Yang, Performance and kinetics study for low-temperature SCR of NO with NH_3 over MnO_x–CeO_2 catalyst, Journal of Catalysis 217 (2003) 434–441.
[15] Y.S. Shen, S.M. Zhu, T. Qiu, et al., A novel catalyst of CeO_2/Al_2O_3 for selective catalytic reduction of NO by NH_3, Catalysis Communications 11 (2009) 20–23.
[16] Z.C. Si, D. Weng, X.D. Wu, et al., Modifications of CeO_2–ZrO_2 solid solutions by nickel and sulfate as catalysts for NO reduction with ammonia in excess O_2, Catalysis Communications 11 (2010) 1045–1048.
[17] H.D. Liu, L.Q. Wei, R.L. Yue, et al., CrO_x–CeO_2 binary oxide as a superior catalyst for NO reduction with NH_3 at low temperature in presence of CO, Catalysis Communications 11 (2010) 829–833.
[18] Z.B. Wu, R.B. Jin, H.Q. Wang, et al., Effect of ceria doping on SO_2 resistance of Mn/TiO_2 for selective catalytic reduction of NO with NH_3 at low temperature, Catalysis Communications 10 (2009) 935–939.
[19] X.D. Wu, Z.C. Si, G. Li, et al., Effects of cerium and vanadium on the activity and selectivity of MnO_x–TiO_2 catalyst for low-temperature NH_3-SCR, Journal of Rare Earths 29 (1) (2011) 64–68.
[20] L. Chen, J.H. Li, M.F. Ge, et al., Mechanism of selective catalytic reduction of NO_x with NH_3 over CeO_2–WO_3 catalysts, Chinese Journal of Catalysis 32 (2011) 836–841.
[21] L. Chen, J.H. Li, M.F. Ge, Promotional effect of Ce-doped V_2O_5–WO_3/TiO_2 with low vanadium loadings for selective catalytic reduction of NO_x by NH_3, Journal of Physical Chemistry C 113 (2009) 21177–21184.
[22] E. Tronconi, I. Nova, C. Ciardelli, et al., Redox features in the catalytic mechanism of the "standard" and "fast" NH_3-SCR of NO_x over a V-based catalyst investigated by dynamic methods, Journal of Catalysis 245 (2007) 1–10.
[23] S. Djerad, M. Crocoll, S. Kureti, et al., Effect of oxygen concentration on the NO_x reduction with ammonia over V_2O_5–WO_3/TiO_2 catalyst, Catalysis Today 113 (2006) 208–214.
[24] R.A. Searles, Pollution from nitric acid plants. Purification of tail gas using platinum catalysts, Platinum Metal Review 17 (2) (1973) 57–63.
[25] G. Qi, R.T. Yang, Low-temperature selective catalytic reduction of NO with NH_3 over iron and manganese oxides supported on titania, Applied Catalysis B: Environmental 44 (2003) 217–225.
[26] W.Q. Xu, Y.B. Yu, C.B. Zhang, et al., Selective catalytic reduction of NO by NH_3 over a Ce/TiO_2 catalyst, Catalysis Communications 9 (2008) 1453–1457.
[27] A. Banerji, V. Grover, V. Sathe, et al., CeO_2–Gd_2O_3 system: unraveling of microscopic features by Raman spectroscopy, Solid State Communications 149 (2009) 1689–1692.
[28] P.R. Ettireddy, N. Ettireddy, S. Mamedov, et al., Surface characterization studies of TiO_2 supported manganese oxide catalysts for low temperature SCR of NO with NH_3, Applied Catalysis B: Environmental 76 (2007) 123–134.
[29] A. Scholz, B. Schnyder, A. Wokaun, Influence of calcination treatment on the structure of grafted WO_x species on titania, Journal of Molecular Catalysis A: Chemical 138 (1999) 249–261.

[30] X. Gao, Y. Jiang, Y.C. Fu, et al., Preparation and characterization of CeO_2/TiO_2 catalysts for selective catalytic reduction of NO with NH_3, Catalysis Communications 11 (2010) 465–469.
[31] S. Damyanova, C.A. Perez, M. Schmal, et al., Characterization of ceria-coated alumina carrier, Applied Catalysis A: General 234 (2002) 271–282.
[32] Q. Wan, L. Duan, K.B. He, et al., Removal of gaseous elemental mercury over a CeO_2–WO_3/TiO_2 nanocomposite in simulated coal-fired flue gas, Chemical Engineering Journal 170 (2011) 512–517.
[33] D.K. Sun, Q.Y. liu, Z.Y. liu, et al., Adsorption and oxidation of NH_3 over V_2O_5/AC surface, Applied Catalysis B: Environmental 92 (2009) 462–467.
[34] M.A. Larrubia, G. Ramis, G. Busca, An FT-IR study of the adsorption of urea and ammonia over V_2O_5–MoO_3–TiO_2 SCR catalysts, Applied Catalysis B: Environmental 27 (2000) L145–L151.
[35] L. Chen, J.H. Li, M.F. Ge, The poisoning effect of alkali metals doping over nano V_2O_5–WO_3/TiO_2 catalysts on selective catalytic reduction of NO_x by NH_3, Chemical Engineering Journal 170 (2011) 531–537.
[36] M.A. Larrubia, G. Ramis, G. Busca, An FT-IR study of the adsorption and oxidation of N-containing compounds over Fe_2O_3–TiO_2 SCR catalysts, Applied Catalysis B: Environmental 30 (2001) 101–110.
[37] L. Chen, J.H. Li, M.F. Ge, et al., DRIFT study on cerium tungsten/titiania catalyst for selective catalytic reduction of NO_x with NH_3, Environmental Science and Technology 44 (2010) 9590–9596.
[38] Z.C. Si, D. Weng, X.D. Wu, et al., Roles of Lewis and Brønsted acid sites in NO reduction with ammonia on CeO_2–ZrO_2–NiO–SO_4^{2-} catalyst, Journal of Rare Earths 28 (2010) 727–731.
[39] W.P. Shan, F. Liu, H. He, et al., A superior Ce–W–Ti mixed oxide catalyst for the selective catalytic reduction of NO_x with NH_3, Applied Catalysis B: Environmental 115–116 (2012) 100–106.
[40] P.W. Seo, S.P. Cho, S.H. Hong, et al., The influence of lattice oxygen in titania on selective catalytic reduction in the low temperature region, Applied Catalysis A: General 380 (2010) 21–27.
[41] Z.C. Si, D. Weng, X.D. Wu, et al., NH_3-SCR activity, hydrothermal stability, sulfur resistance and regeneration of $Ce_{0.75}Zr_{0.25}O_2$–PO_4^{3-} catalyst, Catalysis Communications 17 (2012) 146–149.